Spectral comparisons for different dissipation schemes in WAVEWATCH III

Georgia D. Kalantzi[(1)], Christine Gommenginger, Meric Sroksz
National Oceanography Centre, Southampton, UK

Fabrice Ardhuin
Service Hydrographique et Oceanographique de la Marine, Brest France

1. Introduction

a. Spectral dissipation in numerical models

The real breakthrough in the context of wave modelling came with the introduction of the wave spectrum concept (Pierson *et al*., 1955). The subsequent and very important step was made, among others, by Gelci *et al*. (1956, 1957) who introduced the concept of a dynamical equation describing the evolution of the spectrum. However, due to lack of a sound theoretical basis at that time, Gelci was restricted to empirical expressions for the net source function governing the wave spectrum transport rate. After the fundamental theories of Phillips (1957) and Miles (1957) had been published and the source function for the nonlinear transfer had been derived (Hasselmann, 1962), it became possible to develop the general expression for the source function (Hasselmann, 1962). Roughly, this function consists of three terms: i) the wind input, ii) the nonlinear wave-wave energy transfer and iii) the dissipation by whitecapping; for the case of shallow water an additional term corresponding to bottom friction dissipation, is also added. The source function for deep water may be represented as a superposition of the latter source terms:

$$S = S_{in} + S_{nl} + S_{dis} \,. \quad (1)$$

Spectral dissipation is the least well understood part of all physical processes included in today's wave models (Cavaleri *et al*., 2007). The primary source of spectral wave dissipation is considered to be wave breaking (white-capping), but the physics of this process do not, in any case, have an established validity for all regions and conditions.

Currently, there is much research activity within the field of spectral wave dissipation mainly in connection with the physical aspects of wave breaking through experimental studies. Recent field observations combined with spectral wave analyses (among others, Gemmrich and Farmer, 1999; Banner *et al*., 2000; Babanin *et al*., 2001; Banner *et al*., 2002, Song and Banner, 2004) indicate a 'threshold-like' behaviour of breaking probabilities (see for example Banner *et al*., 2000) related to the spectral steepness across the wave spectrum, but these results have yet to be implemented in operational models; the current formulations are often 'tuning knobs' even in the simplest cases (Cavaleri *et al*., 2007).

The state of the theoretical and experimental knowledge of spectral dissipation is so uncertain that spectral wave modelling is actually following its own way on that

(1) Corresponding author address: Georgia Kalantzi, National Oceanography Centre, Southampton, SO14 3ZH, Southampton, UK. E-mail: gxk@noc.soton.ac.uk

matter. To fill the knowledge gap, the spectral dissipation function is actually estimated as a residual term by the process of tuning the balance of better known source terms and in order to fit known wave spectrum features (Cavaleri *et al*., 2007). One would expect that applications (numerical simulations in wave models) would follow theoretical and/or experimental findings. In this case, all three areas (theoretical research, experimental research and modelling) seem to point in different directions; a discrepancy that does not help towards a unified, universal and sound expression of spectral wave dissipation.

b. Experimental research

Experimental investigations of the spectral dissipation are, actually, very recent: Donelan (2001), Phillips *et al*. (2001), Melville and Matusov (2002), Hwang and Wang (2004), Babanin and Young (2005), Young and Bababin (2006), Babanin *et al*. (2007a,b) are some of the first to deal with the extraction of spectral dissipation functions on the basis of field measurements.

Of the above the only experimental dissipation functions which cover the entire spectral frequency band are the ones proposed by Donelan (2001) and by Young and Babanin (2006); see also Babanin *et al*. (2007a,b). Both include a common feature; a cumulative term that relates dissipation due to whitecapping at smaller scales to features present at larger scales. This "two-phase" (or two-scale) behaviour was also confirmed by independent means in the works of Babanin and Young (2005) and Manasseh *et al*. (2006).

Most of the experimental evidence indicates that the dissipation function is likely not to be local in wavenumber space and is rather a function of the wave spectrum (Cavaleri *et al*., 2007). The most recent findings on formulations of spectral dissipation come to support the two-fold character of spectral dissipation (i.e. i. below) threshold behaviour and ii) cumulative effect) and are included in the companion papers Babanin *et al*. (2007a,b) which mainly follow the work of Young and Babanin (2006).

To conclude this section we highlight the following points:

- there is no consensus among analytical theories of the spectral dissipation of wave energy due to wave breaking, even with respect to the basic characteristics of the dissipation function,
- the theoretical dissipation functions disagree with the experiments,
- contrary to the theory of dissipation, recent experimental advances in wave dissipation studies have brought much more certainty on the behaviour of S_{dis} ,
- approximately over the past decade many physical features of the dissipation process were discovered experimentally and described; among them:
  i. the threshold behaviour of wave breaking (Banner *et al*., 2000; Babanin *et al*., 2001; Banner *et al*., 2002)
  ii. the cumulative effect of wave dissipation at smaller scales (Donelan, 2001; Babanin and Young, 2005; Young and Babanin, 2006),
  iii. the quasi-singular behavior of the dissipation in the middle wavelength range (Hwang and Wang, 2004),
  iv. the two-phase behavior of the dissipation (Babanin and Young, 2005; Manasseh *et al*., 2006), and
  v. the alteration of wave breaking/dissipation at strong wind forcing (Babanin and Young, 2005).

c. Motivation

Taking into consideration what is mentioned in the previous sub-section, and based on the results of Kalantzi *et al*., 2009, where the two of the input/dissipation source term packages of WAVEWATCH III v. 2.22 (Tolman, 2002) were tested for specific wind/wave conditions in the North Indian Ocean, we felt that we needed to further investigate the spectral behavior of these dissipation terms under controlled simple test cases. In that work, we compared wave model parameters such as H_s with altimeter measurements and we found great discrepancies for a period during which the area of North Indian Ocean is mostly dominated by swell seas.

Moreover, since the majority of modeled dissipation terms are parameterized as "tuning knobs" to simply close the wave energy balance, we aimed to test a completely independent source term in the model; a dissipation term based on no previous attempt of model tuning. For that reason we choose the new dissipation term of Babanin *et al*. (2007), which is the result of a field experimental study. The experiment took place at Lake George in Australia and allowed simultaneous measurements of the source functions in a broad range of conditions, including extreme wind-wave conditions (see Section 4).

2. Paper Outline

In the next section the source term packages included in WAVEWATCH III™ v. 3.14, are described in detail. In Section 4, the newly implemented in WAVEWATCH III by the authors, dissipation source term of Babanin *et al*. (2007) (**from now on BAB**), is presented. Section 5 includes the methodology and the results, while Sections 6 and 7 include the discussion on the results and some concluding results, respectively.

3. WAVEWATCH III™ v. 3.14 – Wind input/Dissipation schemes

WAVEWATCH III™ v. 3.14 (from now on WWATCH III; Tolman, 2009) is a full-spectral third generation wind-wave model. It has been developed at the Marine Modeling and Analysis Branch (MMAB) of the Environmental Modeling Center (EMC) of the National Centers for Environmental Prediction (NCEP) and is distributed freely from NCEP's webpage (http://polar.ncep.noaa.gov/waves). The model's code is modular and is operated by switches which allow the user to choose specific model options for each run. In WWATCH III the input and dissipation source terms are treated as a package (share the same switch) and the model provides three options (switches; for further details on the source terms see next section):

- The input/dissipation source terms of WAM cycles 1 through 3 (**from now on WAM3**),
- The source term package of Tolman & Chalikov (1996; **from now on TC96**)

- The source term package of WAM Cycle 4 which includes parameterizations of Bidlot *et al*. (2005; **from now on BAJ**) and Ardhuin *et al*. (2009; **from now on ACC405**).

The following review of the terms, is primarily based on the most recent manual of the model; i.e Tolman, (2009).

a. The WAM3 dissipation source term

The input and dissipation source terms of WAM cycles 1-3 are based on Snyder *et al*. (1981) and Komen *et al*. (1984); see also WAMDIG, (1988). The dissipation source term is this case is given as

$$S_{dis}\left(k,\theta\right)=C_{dis}\hat{\sigma}\frac{k}{\hat{k}}\left(\frac{\hat{a}}{\hat{a}_{PM}}\right)^{2}N\left(k,\theta\right),\ (2)$$

where C_{dis} is a constant, σ the radian frequency, k is the wavenumber, a is the wave steepness, $\hat{a}_{PM}$ is the value of $\hat{a}$ for a Pierson Moskowitz (PM) spectrum, g is the gravitational acceleration, and $N\left(k,\theta\right)$ is the parametric tail of the action spectrum.

b. TC96 source term package

The source term package of Tolman and Chalikov (1996) consists of the input source term of Chalikov and Belevich (1993) and Chalikov (1995), and two dissipation constituents. The (dominant) low-frequency constituent is based on an analogy with energy dissipation due to turbulence

$$S_{dis,l}\left(k,\theta\right)=-2u_{*}hk^{2}\phi N\left(k,\theta\right),\ (3)$$

where h is a mixing scale determined from the high-frequency energy content of the wave field and ϕ is an empirical function accounting for the development stage of the wave field. The empirical high-frequency dissipation is defined as

$$S_{dis,h}\left(k,\theta\right)=-a_{0}\left(\frac{u_{*}}{g}\right)^{2}f^{3}\alpha_{n}^{B}N\left(k,\theta\right),\ (4)$$

where α_n is Phillips' non-dimensional high-frequency energy level normalized by α_r, and where a_0 through a_2 and a_r are empirical constants. $N\left(k,\theta\right)$ is the parametric tail of the action spectrum. u_* and f are the wind friction velocity and frequency, respectively.

It should be noted that in the model eq. (4) is solved by assuming a deep water dispersion relation. The two constituents of the dissipation source term are combined using a simple linear combination, defined by the frequencies f_1 and f_2:

$$S_{dis}\left(k,\theta\right)=AS_{dis,l}+(1-A)S_{dis,h},\ (5)$$

$$A=\begin{cases}1 & \text{for} \quad f<f_{l}\\ \dfrac{f-f_{2}}{f_{1}-f_{2}} & \text{for} \quad f_{1}\le f<f_{2}\\ 0 & \text{for} \quad f_{2}\le f\end{cases}.\ (6)$$

c. WAM4 source term package and variants

These wind-wave interaction source terms are based on the wave growth theory of Miles (1957), modified by Janssen (1982). The pressure-slope correlations

that give rise to part of the wave generation are parameterized following Janssen (1991). A wave dissipation term due to shear stresses variations in phase with the orbital velocity is added for the swell part of the spectrum, based on the swell decay observations of Ardhuin *et al*. (2009).
This parameterization was further extended by Abdalla and Bidlot (2002) to take into consideration a stronger gustiness in unstable atmospheric conditions. Efforts have been made to make the present implementation as close as possible to the one in the ECWAM model (Bidlot *et al*., 2005).

Due to the increase in high frequency input compared to WAM3, the dissipation function was adapted by Janssen (1994) from the WAM3 dissipation, and later reshaped by Bidlot *et al.* (2005). The generic form of the WAM4 dissipation term is,

$$S_{ds}\left(k,\theta\right)^{WAM} = C_{ds}\overline{a}^{2}\overline{\sigma}^{2}\left[\delta_1\frac{k}{\overline{k}}+\delta_2\left(\frac{k}{\overline{k}}\right)^{2}\right]N\left(k,\theta\right), \quad (7)$$

where C_{ds} is a non-dimensional constant and δ_1 and δ_2 are weight parameters, p a constant power, σ the radian frequency, k the wavenumber, a the steepness and $N\left(k,\theta\right)$ the parametric tail of the action spectrum.

The evidence of a threshold behavior of the wave breaking process, the underestimation of swell dissipation (Tolman, 2002f), the very strong dissipation at high frequency given by eq. (19), and the known deficiencies of WAM4 and BAJ source terms in the presence of swell (see e.g. Ardhuin *et al*., 2009) has lead to several new parameterizations. The source term code was thus generalized to allow the use of WAM4, BAJ or other parameterizations (such as ACC405; see Ardhuin *et al*., 2009), via changing the relevant parameters. Hence, the general form of the dissipation source terms computed, takes the form of a combination of a WAM4-type term and a saturation-based term

$$S_{ds} = S_{ds}^{SAT} + S_{ds}^{TURB} + C_{lf}\frac{1-S}{2}S_{ds}^{WAM\,4} + C_{hf}\frac{1+S}{2}S_{ds}^{WAM\,4}. \quad (8)$$

The switch coefficients C_{lf} and C_{hf} allow the switching on and off of either the low (unsaturated) and/or high (saturated) part of the WAM4 dissipation term All relevant source term parameters can be set via the appropriate parameter lists within the model (see Tolman, 2009). The saturation term is given as

$$\begin{aligned} S_{ds}^{SAT}\left(k,\theta\right) = \sigma C_{ds}^{SAT}\Bigg\{ & C_{ds,6}\left[\max\left\{\frac{B\left(k\right)}{B_r P\left(kD\right)}-B_0,0\right\}\right]^{p^{sat}} \\ & +\left(1-C_{ds,6}\right)\left[\max\left\{\frac{B'\left(k\right)}{B_r P\left(kD\right)}-B_0,0\right\}\right]^{p^{sat}}\Bigg\} N\left(k,\theta\right) \end{aligned} \quad . \quad (9)$$

where B is the integrated saturation spectrum, defined as

$$B\left(k\right) = \int_0^{2\pi}\sigma k^3 A\left(k,\theta\right)d\theta \quad (10)$$

and B' is the partially integrated saturation spectrum, defined as

$$B\left(k\right) = \int_{\theta-\Delta\theta}^{\theta+\Delta\theta}\sigma k^3 A\left(k,\theta\right)d\theta', \quad (11)$$

Where θ is the direction and $A(k,\theta)$ the saturation spectrum.

Finally, the wave-turbulence interaction term of Texeira and Belcher (2002) and Ardhuin and Jenkins (2006), is given by

$$S_{ds}^{TURB}(k,\theta) = -2C_{turb}\sigma\cos(\theta_u - \theta)k\frac{\rho_a u_*^2}{\rho_w g}N(k,\theta). \quad (12)$$

The coefficient C_{turb} is of the order of 1 and can be used to adjust for ocean stratification and wave groupiness. In the last expression g is the gravitational acceleration, ρ_a and ρ_w the air and water density, respectively, u_* the wind friction velocity and $N(k,\theta)$ the parametric tail of the action spectrum.

4. Babanin *et al.* (2007) dissipation source term

Within this work we managed to modify and compile the source code of WAVEWATCH^{TM} III, v. 3.14 to implement Babanin *et al.* (2007) new and experimental dissipation term. This term is paired with Tolman and Chalikov's (1996) wind input term.

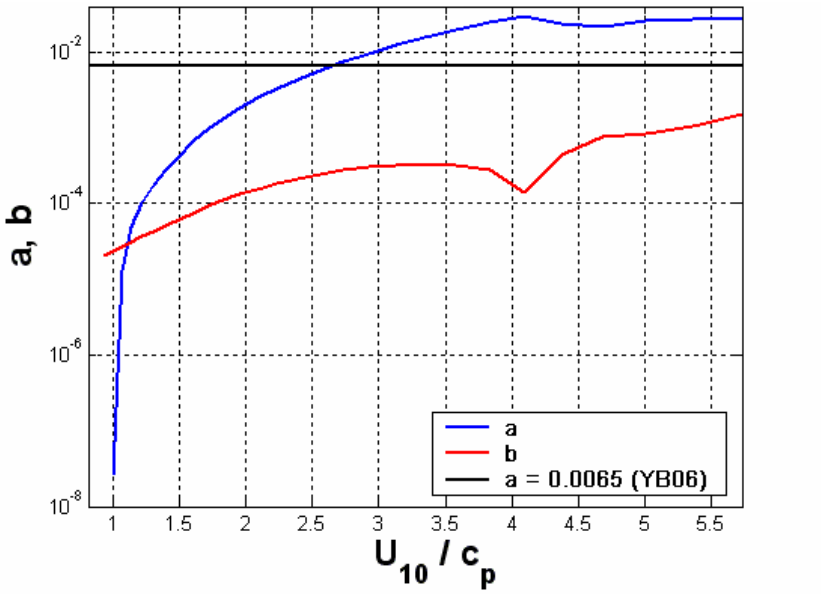

FIGURE 1. Dependence of coefficients $a_1 = a$ (top, blue line) and $a_2 = b$ (bottom, red line) on the wave development stage U_{10}/C_p (Babanin *et al.*, 2007)

Babanin *et al.* (2007a) conducted a field experimental study of wave energy dissipation. The experiment took place at Lake George in Australia and allowed simultaneous measurements of the source functions in a broad range of conditions, including extreme wind-wave circumstances. For the first time, they managed to measure directly the spectral dissipation and they derived frequency distributions both for the wave breaking probability and the breaking severity. Through their experiment they demonstrated that the breaking of waves at a particular frequency causes energy damping in a broad spectral band above that frequency and thus causes a cumulative

dissipative effect for waves of smaller scales. At the small scales (high frequencies), this cumulative dissipation appears to dominate compared to inherent wave-breaking dissipation. Moreover, Babanin *et al*. (2007a) found that at moderate winds the dissipation is fully determined by the wave spectrum whereas at strong winds it is also a function of the wind speed. This result indicates that at extreme wind-forcing conditions a significant part of the extra energy flux is dissipated locally rather than being available for enhancing the wave growth.

The dissipation function of Babanin *et al*. (2007a,b) follows the function proposed in Babanin and Young (2005) and Young and Babanin (2006) and is of the following form:

$$S_{ds}(f) = -a_1 \rho_w g f \left[\left(F(f) - F_{thr}(f) \right) A(f) \right]^n - a_2 \rho_w g \int_{f_p}^{f} \left[\left(F(q) - F_{thr}(q) \right) A(q) \right]^n dq \quad (13)$$

where ρ_w is the water density, g is the gravitational constant, $A(f)$ is the integral characteristic of the inverse directional spectral width (Babanin and Soloviev, 1998a):

$$A(f)^{-1} = \int_{-\pi}^{\pi} K(f,\phi) d\phi \,, \quad (14)$$

where ϕ is the wave direction, $K(f,\phi)$ is the normalized directional spectrum:

$$K(f,\phi_{\max}) = 1 \,, \quad (15)$$

a_i are experimental constants yet to be comprehensively estimated and $F_{thr}(f)$ is the spectral threshold function.

Essentially, a_1 and a_2 determine the spectral level of the wave dissipation source term; a_1 controls the 'inherent' wave breaking term and a_2 the 'induced' dissipation term. The two phase behaviour of this dissipation function represented by these two terms (eq. 13) creates an additional complexity in determining the correct levels of the dissipation wave energy; i.e. in determining the relative contribution of each of those terms. To estimate these coefficients for their specific experimental data, Babanin *et al*. (2007) used a balance of the wind input and dissipation below the spectral peak in a broad range of wave development stages of $U_{10}/C_p = 0.8 - 5.7$, where U_{10} is the wind speed at 10 m height and C_p is the phase speed of the spectral-peak waves (see Fig. 1). They clearly note, however, that this issue has to be extensively revisited, especially since this estimation is mostly based on the wind input and hence a_1 and a_2 are most probably sensitive to the choice of the wind input source term to be paired with he dissipation one within the model.

Moreover, in their study a linear dissipation $n = 1$ was employed which is consistent dimensionally, agrees with measurements by Young and Babanin (2006) and seems the best suitable for satisfying the physical constraints in the numerical simulations.

The most significant uncertainty in the dissipation function (eq. 13) is the unknown threshold spectrum $F_{thr}(f)$. Babanin and Young (2005) investigated this threshold in dimensionless terms; that is in terms of the saturation spectrum $\sigma(f)$ normalized by the directional spectrum parameter in eq. (14):

$$\sigma(f) = \sigma_{Phillips}(f) A(f) \,, \quad (16)$$

where $\sigma_{Phillips}(f)$ is as introduced in Phillips (1984):

$$\sigma_{Phillips}(f) = \frac{(2\pi)^4 f^5 F(f)}{2g^2}. \quad (17)$$

If a universal dimensionless saturation-threshold value σ_{thr} (proposed in Babanin *et al*., 2007 as $\sqrt{\sigma_{thr}} = \text{const} = 0.035$) can be established, the dimensional threshold can then be obtained at every frequency as:

$$F_{thr} = \frac{2g^2\sigma_{thr}}{(2\pi)^4 A(f) f^5}. \quad (18)$$

In order to implement the expression of eq. (13) in WWATCH III, we had to convert this frequency dependent dissipation spectrum into a wavenumber-direction spectrum. Hence, the corresponding expression that we used in the model is of the following form:

$$S_{ds}(k,\theta) = -\left[a_1 \rho_w g f \left[\left(F(f) - F_{thr}(f) \right) A(f) \right]^n \right.$$
$$\left. - a_2 \rho_w g \int_{f_p}^{f} \left[\left(F(q) - F_{thr}(q) \right) A(q) \right]^n dq \right] \frac{F(f,k)}{F(f)} \frac{2\pi}{C_g}. \quad (19)$$

5. Results

a. The approach

We aim to investigate the behaviour of WWATCH III and specifically of its different wind input/dissipation schemes in simple and controlled point test cases, along with the newly implemented by the authors, dissipation source term of Babanin *et al*. (2007).

As mentioned in Section 3, the new version of the model includes three options of wind input/dissipation source term packages:

- The input/dissipation source terms of WAM cycles 1 through 3 (WAM3).
- The source term package of Tolman & Chalikov (1996) (TC96).
- The source term package of WAM cycle 4. Due to the increase in high frequency input compared to WAM3, the dissipation function was adapted by Janssen (1994) and later reshaped by Bidlot *et al*. (2005) (BAJ). Moreover, the latest evidence of a threshold behaviour of the wave breaking process, the very strong dissipation at high frequency and the deficiencies of WAM cycle 4 and BAJ source terms in the presence of swell has led to attempts of new parameterisations. One of them is under development by Ardhuin F. and his team and is included in these tests (ACC405, see Ardhuin *et al*., 2009)

Each term was tested in simple test runs at one grid point with idealised wind and wave forcing for each run; i.e., wind speed of: 10 m/sec, and wave height of the initial field of: 0 and 3 m. The initial field type was Gaussian in frequency and space, and cosine type in direction, while the runs were set up for 30 frequencies from 0.0412 to 0.6530, and 36 directions. The initial wave field's direction was set to 90^o and the wind's direction to 270^o. The time of the model runs was 96 hours so the wave field can be considered as fully developed.

For each run and each dissipation term, we examined the one-dimensional dissipation spectrum and we plot the results for a specific combination of initial wave field and wind speed (e.g. 0 m initial wave field and 10 m/sec wind speed), with respect to frequency or f/f_p. Also we present the evolution of the one-dimensional dissipation spectrum for BAB, from zero time up to 96 hours, again for the two combinations of initial wave field and wind speed.

It has to be noted that this preliminary work does not aim to tune the new BAB source term in the model. It is a simple test, which provides information via comparison, on the existing WWATCH III dissipation terms along with a new and experimental one.

For reference, we chose all the parameters to be as suggested in Babanin *et al*. (2007), except for the values of a_1 and a_2; i.e $n=1$ and $\sqrt{\sigma_{thr}}=0.035$. The choice of these values for the present work was based solely on the scale comparison with the one-dimensional dissipation spectrum of the rest of the terms; namely ACC405, BAJ, WAM3 and TC96 (for abbreviation see Section 2 and 3). The values that we chose here are $a_1=10^{-5}$ and $a_2=10^{-7}$. Bearing in mind that the wave development stage of our test cases is approximately $U_{10}/C_p \sim 1$, the latter values of a_1 and a_2, do not seem to agree with Fig. 1. However, let's recall that these coefficients in Fig. 1 were estimated for a specific experimental dataset and a specific wind input (balanced with the dissipation below the spectral peak); hence the use of a different wind input term herein (BAB term is paired with the corresponding wind input term of TC96), as well as the simulated model cases that we use, might be the source of this difference. In any case it is clear that these matters need further investigation.

b. Plots

In this subsection the plots of the results we acquired, are presented. Detailed comments on these results follow in the next Section.

Fig. 2 and 3 present the one-dimensional dissipation spectra of all the source terms examined herein (namely, ACC405, BAJ, WAM3, TC96 and BAB), for initial condition combinations of 0 m initial wave field – 10 m/sec wind speed and 3 m initial wave field – 10 m/sec wind speed, respectively. For both cases the spectra are plotted against frequency and refer to the 96th hour of the associated runs. Fig. 4 and 5 present exactly the same results as Fig. 2 and 3 only this time dissipation spectra are plotted against f/f_p. Fig. 6 presents the one-dimensional dissipation spectra of the source terms for the case of 3 m initial wave field – 10 m/sec wind speed and refers to the 48th hour of the associated model runs.

Finally, Fig. 7 and 8 present the time evolution of the one-dimensional dissipation spectra acquired with BAB source term, for initial condition combinations of 0 m initial wave field – 10 m/sec wind speed and 3 m initial wave field – 10 m/sec wind speed, respectively. In both cases the dissipation spectra are plotted against frequency and they refer to zero up to the 96th hour of the associated models runs. It should be noted that in these plots time evolves from low to high line density; roughly from high to lower frequencies.

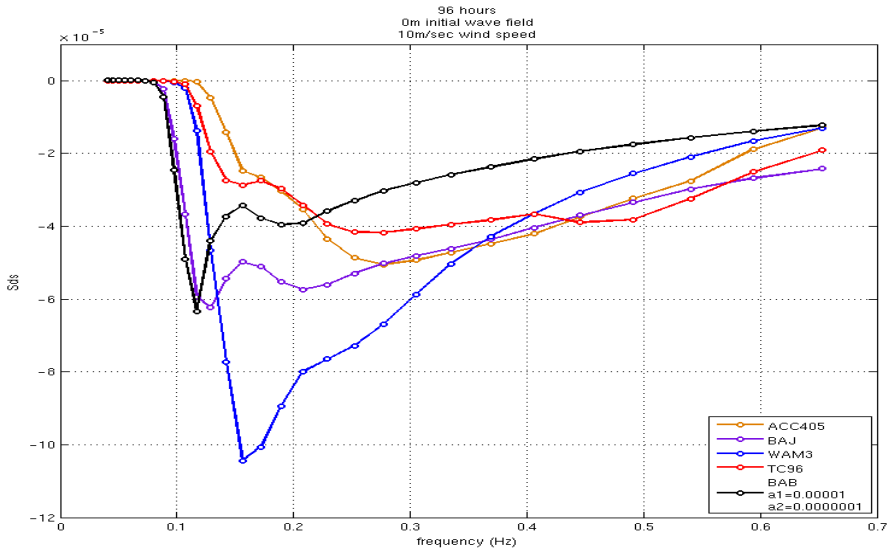

FIGURE 2. One-dimensional dissipation spectra for the source terms examined, plotted against frequency, at 96 hours. The plot corresponds to 0 m initial wave field and 10 m/sec wind speed.

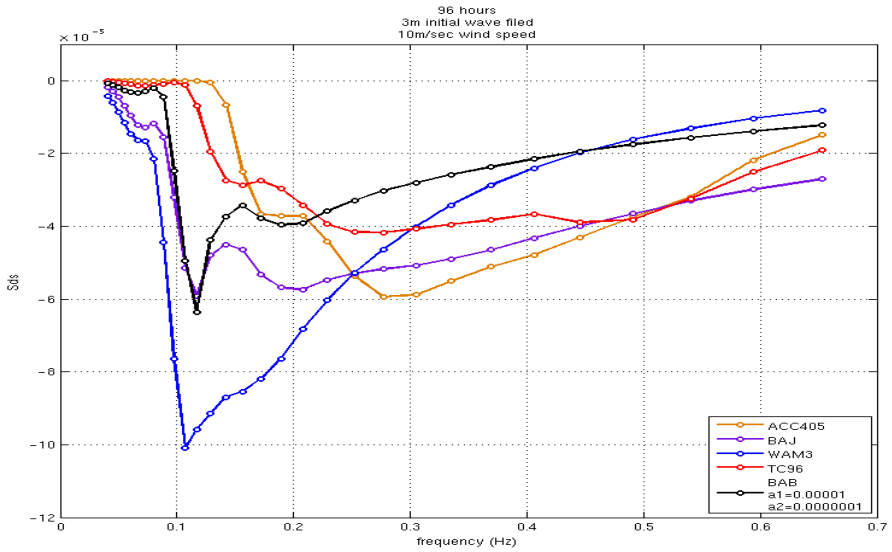

FIGURE 3. One-dimensional dissipation spectra for the source terms examined, plotted against frequency, at 96 hours. The plot corresponds to 3 m initial wave field and 10 m/sec wind speed.

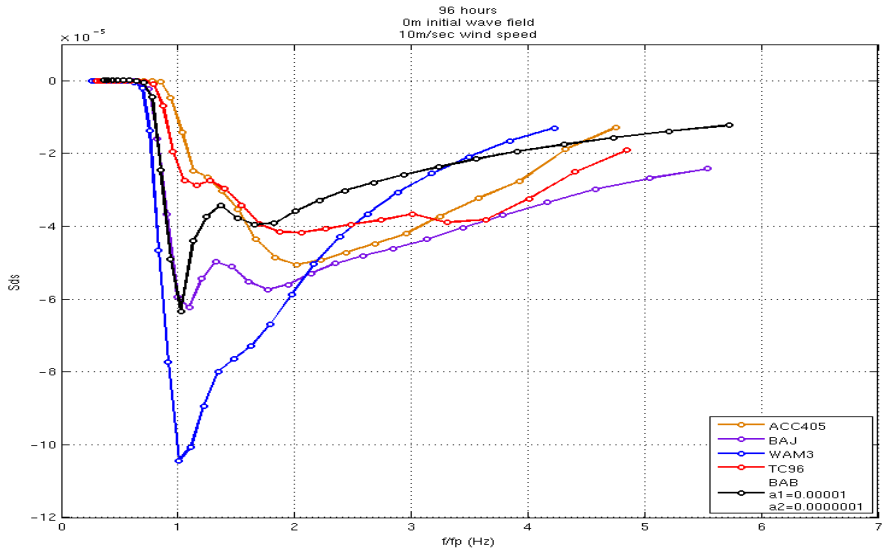

FIGURE 4. One-dimensional dissipation spectra for the source terms examined plotted against f/f_p, at 96 hours. The plot corresponds to 0 m initial wave field and 10 m/sec wind speed.

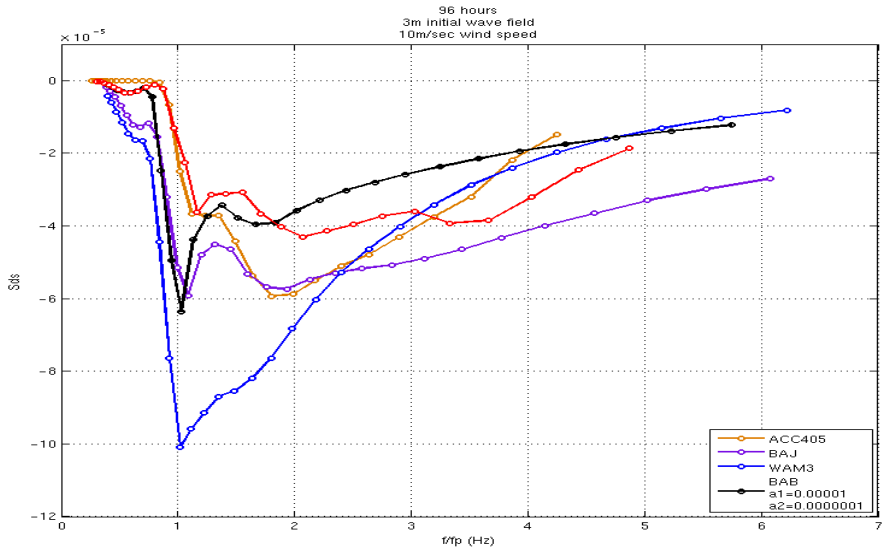

FIGURE 5. One-dimensional dissipation spectra for the source terms examined plotted against f/f_p, at 96 hours. The plot corresponds to 3 m initial wave field and 10 m/sec wind speed.

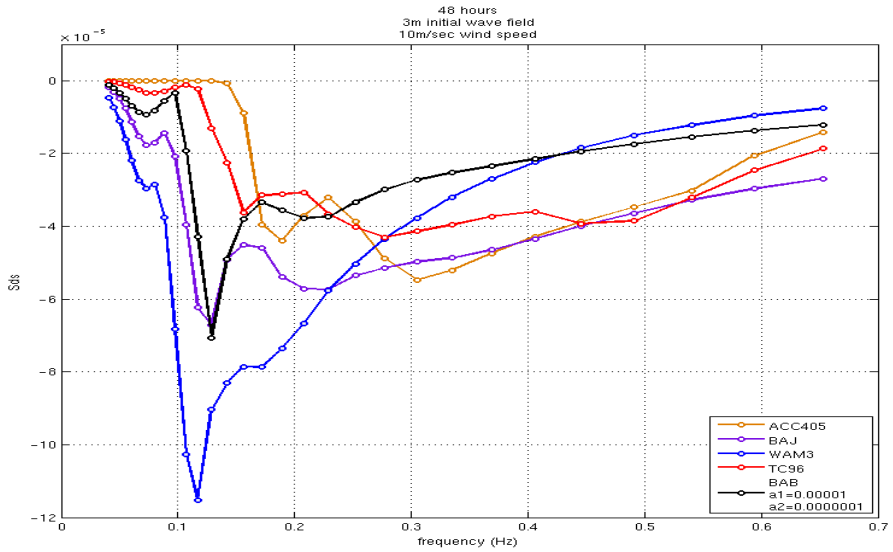

FIGURE 6. One-dimensional dissipation spectra of the source terms examined plotted against frequency, 48 hours. The plot corresponds to 3 m initial wave field and 10 m/sec wind speed

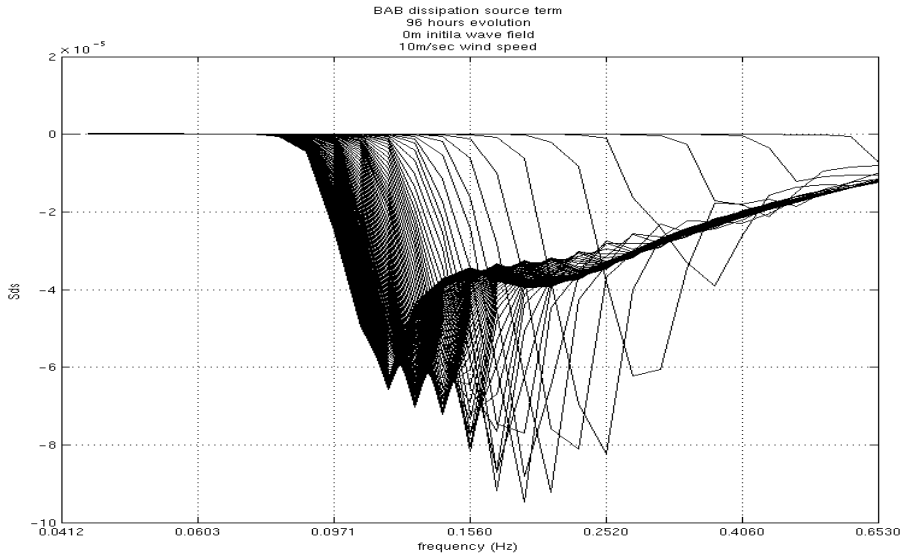

FIGURE 7. Evolution of the one-dimensional dissipation spectra of BAB term from zero time to 96 hours. The spectra are plotted against frequency and the time evolution progresses from the lower to the higher line density. The plot corresponds to 0 m initial wave field and 10 m/sec wind speed.

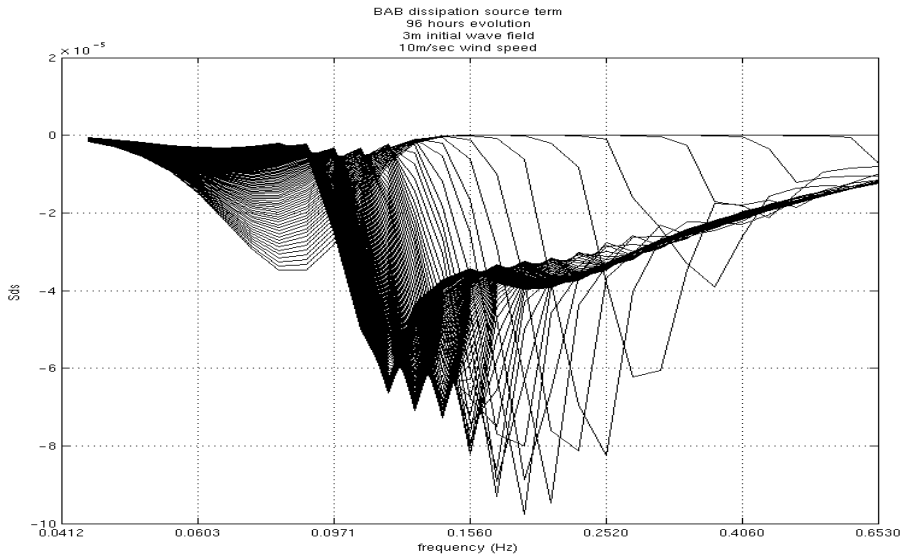

FIGURE 8. Evolution of the one-dimensional dissipation spectra of BAB term from zero time to 96 hours. The spectra are plotted against frequency and the time evolution progresses from the lower to the higher line density. The plot corresponds to 3 m initial wave field and 10 m/sec wind speed.

6. Discussion

From Fig. 2 it can be easily seen that all five source terms produce quite different dissipation spectral shapes. In this case the initial wave field was set to zero, so the results correspond only to wind sea. Most of the terms have their dissipation peak at different frequencies. Specifically, the peak dissipation of BAB is at ~0.12 Hz, BAJ at ~0.13 Hz, WAM3 at ~0.15 Hz, and both ACC405 and TC96 at ~0.27 Hz. If we combine these results with Fig. 4, where exactly the same spectra are presented only plotted against f/f_p, we can see that not all terms give their highest dissipation at the peak frequency. BAB, BAJ and WAM3 do give their dissipation peak at f_p, while ACC405 and TC96 give their dissipation peak at $\sim 2f_p$. Shape-wise BAB and BAJ share similar dissipation behaviors; they both peak at f_p, although BAJ gives higher dissipation towards the high frequency tail (difference of the order of $2\text{x}10^{-5}$ to $1\text{x}10^{-5}$ towards higher frequencies). The shapes of ACC405 and TC96 dissipation spectra are also similar, giving comparable dissipation values near f_p and up to $\sim 1.8f_p$ (~0.12 Hz); going to higher frequencies ACC405 gives higher dissipation than TC96 until $\sim 3.2f_p$ (~0.43 Hz), after which TC96 produces more dissipation at the high frequency tail (difference of the order of $1\text{x}10^{-5}$). WAM3 presents a very different shape to all the other terms, giving very high dissipation near f_p (difference of the order of $4\text{x}10^{-5}$ from BAB and BAJ, and of the order of $7\text{x}10^{-5}$ from ACC405 and TC96) and decreasing rapidly towards higher frequencies.

Moving on to Fig. 3 and 5, where the dissipation spectra are plotted against frequency and f/f_p, respectively, for the case of 3 m initial wave field and 10 m/sec wind speed at 96 hours, it can be seen that the shapes are similar to the previous case

(0 m initial wave field – 10 m/sec wind speed) except for the dissipation "lobe" present at frequencies lower than f_p. The latter obviously corresponds to the effect of the initial wave field (swell). An exception to all other terms is ACC405, which does not give any dissipation below f_p, but enhances by ~1x10^{-5} its dissipation peak at $\sim 2f_p$ (~0.27 Hz). All other terms keep their dissipation peak almost intact.

Fig. 6 presents similar results as in Fig. 3, only this time at 48 hours. This was done to demonstrate the time evolution effect on the swell dissipation of the terms examined. In this case, the dissipation "lobes" below the peak frequency are larger and the sequence of higher to lower dissipation at this frequency region is: WAM3, BAJ, BAB, TC96 and ACC405 which gives almost zero dissipation. Again this time ACC405 produces an enhanced dissipation at $\sim 2f_p$ (~0.3 Hz).

Lastly, Fig. 7 and 8 demonstrate the time evolution of the BAB dissipation spectra from zero time to 96 hours, for the cases of 0 m initial wave field – 10 m/sec wind speed and 3 m initial wave field – 10 m/sec wind speed, respectively. The time evolution for both plots progresses from low to higher line density; roughly from high to lower frequencies. The interesting feature of these plots is the effect of the initial wave field (swell) which creates the decreasing over time dissipation "lobe" below the peak frequency (see Fig. 8). However, this effect leaves almost intact the dissipation spectral shapes and magnitudes for frequencies higher than f_p.

7. Conclusion

In this work we aimed to compare the dissipation spectra of five dissipation terms implemented in WAVEWATCH III^{TM} v.3.14 (Tolman, 2009); four of them were already included in this version of the model, while we implemented the fifth one, namely Babanin *et al*. (2007). These comparisons were made for simple test model runs under idealized initial conditions; 0 m initial wave field – 10 m/sec wind speed and 3 m initial wave field – 10 m/sec wind speed. The dissipation spectra that were compared corresponded to the 48th and the 96th hour of the model runs. Apart from the dissipation spectral comparisons from different terms, we examined the time evolution from zero to the 96th hour of BAB's dissipation spectra.

A first remark would be that despite the luck of any previous tuning, Babanin *et al*. (2007) dissipation term gave quite comparable results to all other extensively tuned in the model, terms. However, the choice of the coefficients a_1 and a_2 of BAB's expression in eq. (13) was done quite empirically in this work and this is a matter that needs to be addressed after further investigation. All other coefficients of eq. (13) were set to the values proposed in Babanin et al. (2007).

From the dissipation spectral comparisons it seems that BAB presents similar shape to BAJ, although producing less dissipation for frequencies higher than the peak frequency. Different from those two but quite similar to each other are the shapes of the dissipation spectra of ACC405 and TC96. WAM3 produced dissipation spectral shapes that were very different from all other terms. Another interesting feature is that both ACC405 and TC96 give their dissipation peak not at f_p, where all the other terms do, but at $\sim 2f_p$.

All terms produced a dissipation "lobe" at frequencies lower than f_p, when the initial wave field was set to 3 m (presence of swell). The only exception to the

latter is ACC405 which instead of this "lobe" presented an enhanced by $1x10^{-5}$ dissipation peak at $\sim 2f_p$, when swell is present (initial wave field of 3 m).

Finally the time evolution plots of BAB dissipation spectra reveals that the presence of the initial wave field (3 m) affects neither the shape nor the magnitude of the dissipation spectra above the peak frequency. However, it does produce a decreasing over time dissipation "lobe" at frequencies lower than f_p.

8. References

Abdalla, S. and J. R. Bidlot, 2002: Wind gustiness and air density e_ects and other key changes to wave model in CY25R1. Tech. Rep. Memomrandum R60.9/SA/0273, Research Department, ECMWF, Reading, U. K.

Ardhuin, F., E. Rogers, A. Babanin, J-F. Filipot, R. Magne, A. Roland, A. van der Westhuysen, P. Queffeulou, J-M. Lefevre, L. Aouf, F. Collard, 2009: Semi-empirical dissiaprion source functions for ocean waves: Part I, definition, calibration and validation. *J. Phys. Ocean*, in press.

_____, A. D. Jenkins, 2006: On the interaction of surface waves and upper ocean turbulence. *J. Phys. Ocean*., **36(3)**, 551-557.

Babanin, A.V. and Soloviev, Yu.P. 1998a: Variability of directional spectra of windgenerated waves, studied by means of wave staff arrays. *Marine & Freshwater Res*., **49**, 89-101

_____, I. R., Young, M.L., Banner, 2001: Breaking probabilities for dominant surface waves on water of finite constant depth. *J. Geophys. Res.*, **C106**, 11659-11676.

_____, and I. R., Young, 2005: Two-phase behaviour of the spectral dissipation of wind-waves, *Proc. 5th Int. Symp. WAVES 2005*, 3-7 July, 2005, Madrid, Spain.

_____, _____, R., Manasseh, E., Schultz, 2007a: Spectral dissipation term for wave forecast models, experimental study, *Proc. 10th Int. Workshop on Wave Hindcasting and Forecasting 2007*, 11-16 November, Oahu, Hawaii, USA.

_____, K., Tsagareli, I. R., Young, D., Walker, 2007b: Implementation of new experimental input/dissipation terms for modelling spectral evolution of wind-waves, *Proc. 10th Int. Workshop on Wave Hindcasting and Forecasting 2007*, 11-16 November, Oahu, Hawaii, USA.

Banner, M. L., A. V., Babanin, I. R., Young, 2000: Breaking probability of dominant waves on the sea surface. *J. Phys. Ocean.*, **30**, 3145-3160.

_____, J. R., Gemmrich, D. M., Farmer, 2002: Multi-scale measurements of ocean wave breaking probability. *J. Phys. Ocean.*, **32**, 3364-3375.

Bidlot, J. R., S., Abdalla, P. A. E. M., Janssen, 2005: A revised formulation for ocean wave dissipation in CY25R1. Tech. Rep. Memorandum R60.9/JB/0516, Research Department, ECMWF, Reading, U.K.

Cavaleri, L., J.-H. G. M., Alves, F., Ardhuin, A., Babanin, M., Banner, K., Belibassakis, M., Benoit, M., Donelan, J., Groeneweg, T. H. C., Herbes, P., Hwang, P. A. E. M., Janssen, T., Janssen, I. V., Lavrenov, R., Magne, J., Monbaliu, M., Onorato, V., Polnikov, D., Resio, W. E., Rogers, A., Sheremet, J., McKee Smith, H. L., Tolman, G., van Vledder, J., Wolf, I., Young: The WISE group: 2007: Wave modelling – The state of the art. *Progr. in Ocean.*, **75**, 603-674.

Chalikov, D. V., 1995. The parameterization of the wave boundary layer. *J. Phys. Ocean.*, **25**, 1333-1349.

_____, and M. Y., Belevich, 1993: One-dimensional theory of the wave boundary layer. *Boundary Layer Meteorology*, **63**, 65-96.

Donelan, M., 2001: A nonlinear dissipation function due to wave breaking, *ECMWF Workshop on Ocean Wave Forecasting*, 2-4 July, 2001, Series ECMWF Proceedings, 87-94.

Gelci, R., H., Cazalé, J., Vassal, 1956: Utilization des diagrammes de propagation à la prévision énergétique de la houle. *Bull. Inform. Comité Central Océanogr. Etude Côtes*, **8**, 170-187.

_____, _____, _____, 1957: Prevision. de la houle - La method. des. densites spectroangulaires. *Bull. Inform. Comité Central Océanogr. Etude Côtes*, **9**, 416--435.

Hasselmann, K., 1962: On the non-linear energy transfer in a gravity-wave spectrum, part 1: general theory. *J. Fluid Mech.*, **12**, 481.

Hwang, P. A., and D. W., Wang, 2004: An empirical investigation of source term balance of small scale surface waves". *Geophysical Research Letters*, **31**, L15301, doi: 10.1029/2004GL020080.

Janssen, P. A. E. M., 1982: Quasilinear approximation for the spectrum of wind-generated water waves. *J. Fluid Mech*., **117**, 493-506.

_____, 1991: Quasi linear theory of wind wave generation applied to wave forecasting. *J. Phys. Oceanogr.*, **21**, 1631-1642.

_____, K. Hasselmann, S. Hasselmann, and G. J. Komen, 1994: Parameterization of source terms and the energy balance in a growing wind sea. Dynamics and modelling of ocean waves, G. J. Komen et al., ed., Cambridge University Press, pages 215– 238.

Kalantzi, G.D., C. Gommenginger, M. Srokosz, 2009: Assessing the performance of the dissipation parameterisations in WAVEWATCH III by using collocated altimetry data. *J. Phys. Ocean*, doi: 10.1175/2009JPO4182.1, in press.

Komen, G. J., S., Hasselmann, K., Hasselmann, 1984: On the existence of a fully developed wind-sea spectrum. *J. Phys. Ocean.*, **14**, 1271-1285.

Manasseh, R., A. V., Babanin, C., Forbes, K., Richards, I., Bobevski, A., Ooi, 2006: Passive acoustic determination of wave-breaking events and their severity across the spectrum. *J. Atm. and Ocean. Tech.*, **23(4)**, 599-618.

Melville, W. K., and P., Matusov, 2002: Distribution of breaking waves. *Nature*, **417**, 58-63.

Miles, J. W., 1957: On the generation of surface waves by shear flows. *J. Fluid Mech.*, **3**, 185-204.

Gemmrich, J. R., and D. M., Farmer, 1999: Observations of the scale and occurrence of breaking surface waves. *J. Phys. Ocean.*, **29**, 2595-2606.

Phillips, O. M., 1957: On the generation of waves by turbulent wind. *J. Fluid Mech.*, **2**, 417-445.

_____, F. L., Posner, J. P., Hansen, 2001. High range resolution radar measurements of the speed distribution of breaking events in wind-generated ocean waves: surface impulse and wave energy dissipation rates. *J. Phys. Ocean.*, **31**, 450-460.

Pierson, W. J., G., Neumann, R. W., James, 1955: Practical methods for observing and forecasting ocean waves by means of wave spectra and statistics. *H.O. Pub 603*, US Navy Hydrographic Office, Washington, DC.

Snyder, R. L., F. W., Dobson, J. A., Elliot, R. B., Long, 1981: Array measurements of atmospheric pressure fluctuations above surface gravity waves. *J. Fluid Mech.*, **102**, 1-59.

Song, J., and M. L., Banner, 2004: On the influence of mean water depth and a subsurface sand bar on the onset and strength of wave breaking. *J. Phys. Ocean.*, **34**, 950-960.

Song, J., and M. L., Banner, 2004: On the influence of mean water depth and a subsurface sand bar on the onset and strength of wave breaking. *J. Phys. Ocean.*, **34**, 950-960.

Teixeira, M. A. C. and S. E. Belcher, 2002: On the distortion of turbulence by a progressive surface wave. *J. Fluid Mech*., 458, 229-267.

Tolman, H. L., 2002: User manual and system documentation of WAVEWATCH-III version 2.22. *NOAA / NWS / NCEP / OMB Technical Note*, No. 222, 133 pp.

_____, 2009: User manual and system documentation of WAVEWATCH-III version 3.14. *NOAA / NWS / NCEP / OMB Technical Note*, No. 276, 194 pp.

_____, and D. V., Chalikov, 1996: Source terms in a third generation wind-wave model. *J. Phys. Ocean.*, **26**, 2497-2518.

WAMDI group: S., Hasselmann, K., Hasselmann, E., Bauer, P. A. E. M., Janssen, L., Komen, L., Bertotti, P., Lionello, A., Guillaume, V. C., Cardone, J. A., Greenwood, M., Reistad, L., Zambresky, J. A., Ewing, 1988: The WAM model – a third generation ocean wave prediction model. *J. Phys. Ocean.*, **18**, 1775-1810.

Young, I. R., and A. V., Babanin, 2006: Spectral distribution of energy dissipation of wind-generated waves due to dominant wave breaking. *J. Phys. Ocean.*, **36(3)**, 376-394.